Gd^{III} Complexes with Fast Water Exchange and High Thermodynamic Stability: Potential Building Blocks for High-Relaxivity MRI Contrast Agents**

Sabrina Laus, Robert Ruloff, Éva Tóth, and André E. Merbach*[a]

Abstract: On the basis of structural considerations in the inner sphere of nine-coordinate, monohydrated Gd^{III} poly(aminocarboxylate) complexes, we succeeded in accelerating the water exchange by inducing steric compression around the water binding site. We modified the common $DTPA^{5-}$ ligand (DTPA = (diethylenetriamine-*N*,*N*,*N*′,*N*″,*N*″-pentaacetic acid) by replacing one ($EPTPA^{5-}$) or two ($DPTPA^{5-}$) ethylene bridges of the backbone by propylene bridges, or one coordinating acetate by a propionate arm ($DTTA\text{-}prop^{5-}$). The ligand $EPTPA^{5-}$ was additionally functionalized with a nitrobenzyl linker group ($EPTPA\text{-}bz\text{-}NO_2^{5-}$) to allow for coupling of the chelate to macromolecules. The water exchange rate, determined from a combined variable-temperature ^{17}O NMR and EPR study, is two orders of magnitude higher on $[Gd(eptpa\text{-}bz\text{-}NO_2)(H_2O)]^{2-}$ and $[Gd(eptpa)(H_2O)]^{2-}$ than on $[Gd(dtpa)(H_2O)]^{2-}$ ($k_{ex}^{298} = 150\times10^6$, 330×10^6, and $3.3\times10^6\ s^{-1}$, respectively). This is optimal for attaining maximum proton relaxivities for Gd^{III}-based, macrocyclic MRI contrast agents. The activation volume of the water exchange, measured by variable-pressure ^{17}O NMR spectroscopy, evidences a dissociative interchange mechanism for $[Gd(eptpa)(H_2O)]^{2-}$ ($\Delta V^{\neq} = (+6.6\pm1.0)\ cm^3\,mol^{-1}$). In contrast to $[Gd(eptpa)(H_2O)]^{2-}$, an interchange mechanism is proved for the macrocyclic $[Gd(trita)(H_2O)]^{-}$ ($\Delta V^{\neq} = (-1.5\pm1.0)\ cm^3\,mol^{-1}$), which has one more CH_2 group in the macrocycle than the commercial MRI contrast agent $[Gd(dota)(H_2O)]^{-}$, and for which the elongation of the amine backbone also resulted in a remarkably fast water exchange. When one acetate of $DTPA^{5-}$ is substituted by a propionate, the water exchange rate on the Gd^{III} complex increases by a factor of 10 ($k_{ex}^{298} = 31\times10^6\ s^{-1}$). The $[Gd(dptpa)]^{2-}$ chelate has no inner-sphere water molecule. The protonation constants of the $EPTPA\text{-}bz\text{-}NO_2^{5-}$ and $DPTPA^{5-}$ ligands and the stability constants of their complexes with Gd^{III}, Zn^{II}, Cu^{II} and Ca^{II} were determined by pH potentiometry. Although the thermodynamic stability of $[Gd(eptpa\text{-}bz\text{-}NO_2)(H_2O)]^{2-}$ is reduced to a slight extent in comparison with $[Gd(dtpa)(H_2O)]^{2-}$, it is stable enough to be used in medical diagnostics as an MRI contrast agent. Therefore both this chelate and $[Gd(trita)(H_2O)]^{-}$ are potential building blocks for the development of high-relaxivity macromolecular agents.

Keywords: gadolinium · ligand design · imaging agents · poly(aminocarboxylates)

Introduction

Within the last decade, magnetic resonance imaging (MRI) has evolved into one of the most powerful techniques in medical diagnostics. This development is related to the successful use of paramagnetic agents, mostly Gd^{III} complexes, which enhance the intrinsic contrast, thus contributing to the excellent anatomical resolution of the magnetic resonance images.[1] Some currently emerging MRI applications, particularly molecular imaging, require contrast agents of much higher efficiency than those already marketed.[2] In the case of receptor targeting, biological constraints such as low receptor concentration (10^{-9}–10^{-13} mol g^{-1} of tissue) and receptor saturation are strongly limiting, as Nunn et al. first pointed out.[3] The limitation can be reduced by increasing the relaxivity (efficacy) of the contrast agent, either by greater intrinsic relaxivity or by attaching many paramagnetic centers to the target.[4] Different strategies are currently being tested to deliver many Gd-containing species to the site to be imaged.

High-efficacy agents can only be designed on a rational basis, by considering the relationships between structure,

[a] Prof. A. E. Merbach, S. Laus, Dr. R. Ruloff, Dr. É. Tóth
Institut de Chimie Moléculaire et Biologique
Ecole Polytechnique Fédérale de Lausanne, EPFL-BCH
1015 Lausanne (Switzerland)
Fax: (+41) 21-693-9875
E-mail: andre.merbach@epfl.ch

[**] High-pressure NMR kinetics, Part 101. Part 100: L. Burai, É. Tóth, G. Moreau, A. Sour, R. Scopelliti, A. E. Merbach, *Chem. Eur. J.* **2003**, *9*, 1394.

Supporting information for this article is available on the WWW under http://www.chemeurj.org/ or from the authors.

 DOI: 10.1002/chem.200204612

dynamics and the relevant parameters determining relaxation processes. The relaxivity of a contrast agent is defined as the paramagnetic proton relaxation rate enhancement of the bulk water protons, referred to a 1 mM concentration of gadolinium. The Solomon–Bloembergen–Morgan theory, which relates the observed paramagnetic relaxation rate enhancement to microscopic properties, predicts maximum proton relaxivities for Gd^{III} complexes ($>100\ mM^{-1}s^{-1}$ for monohydrated chelates instead of $4-5\ mM^{-1}s^{-1}$ for commercial agents) when the three most important influencing factors, rotation, electron spin relaxation and water exchange, are optimized simultaneously.[5] The necessity of slowing down the rotation prompted the development of macromolecular agents, involving either covalent or non-covalent binding between the Gd^{III} chelate and the macromolecule. The optimization of the electron spin relaxation on Gd^{III} complexes remains a difficult issue, despite the recent advances in the theoretical description and in the accessibility of experimental EPR data (at variable magnetic fields, measurement of T_{1e}). The peculiarity of the water exchange rate, the third determining factor for proton relaxivity, is that its value has to be in a relatively small range (around $k_{ex}=10^8\ s^{-1}$) in order to attain maximum relaxivities. Water exchange on the currently used Gd^{III}-based contrast agents is about two orders of magnitude slower ($k_{ex}\approx10^6\ s^{-1}$),[5] and its tuning to the optimal value is far from evident. Several examples show that it is easy to slow down the water exchange further by structural modification of the ligand (for example, replacement of carboxylates by amides), but the acceleration of the water exchange is more problematic. Moreover, high thermodynamic and kinetic stability has always to be preserved to ensure non-toxicity of the Gd^{III} complex. Some bishydrated chelates have shown faster water exchange. Recently, the bishydrated Gd^{III} complexes of TREN-Me-3,2-HOPO derivatives were reported as promising candidates for MRI contrast agents, due to their optimal water exchange rate and high thermodynamic stability.[6] However, a potential drawback for bishydrated chelates is their tendency to form ternary complexes in biological fluids that always contain a variety of small coordinating ligands, some of them in considerably high concentration (carbonate, phosphate, citrate). The formation of such ternary complexes would then erase any relaxivity gain in vivo.[7]

Nine-coordinate, monohydrated Gd^{III} poly(aminocarboxylates), including all commercial Gd^{III}-based MRI contrast agents, undergo a dissociative (D), or dissociative-interchange (I_d), water exchange, in contrast to the associative (A) mechanism on $[Gd(H_2O)_8]^{3+}$.[5] The rate of such dissociative exchange processes is determined primarily by the overall charge in the chelate (more negative charge leads to faster exchange) and by the steric crowding around the bound water site. Increasing the negative charge of Gd^{III} complexes which are dedicated to medical use is not viable since it would imply a higher osmotic load. An increased steric compression around the inner-sphere water molecule will facilitate its leaving, which, in a dissociative process, constitutes the rate-determining step. The significance of steric crowding at the water binding site was well demonstrated by an ^{17}O NMR study on the lanthanide series of DTPA-BMA complexes (DTPA-BMA = 1,7-bis[(*N*-methylcarbamoyl)methyl]-1,4,7-tris(carboxymethyl)-1,4,7-triazaheptane).[8] They are all nine-coordinate, with one inner-sphere water molecule. On progression from the middle to the end of the lanthanide series, the eight-coordinate transition state becomes more and more accessible in the dissociative exchange process as the radius of the lanthanide ion decreases. The result is an increase in the water exchange rate by one order of magnitude from [Eu(dtpa-bma)(H_2O)] to [Ho(dtpa-bma)(H_2O)]. On the basis of these observations, we set off with the idea of inducing steric compression around the water binding site in dissociatively exchanging Gd^{III} complexes by small structural modifications of the common poly(aminocarboxylate) ligands in order to accelerate the water exchange without considerably decreasing the complex stability. Recently, in a preliminary communication, we reported the first example of a rationally designed ligand structure that results in a remarkably fast water exchange of the Gd^{III} complex.[9] We increased steric compression around the water binding site in the macrocyclic chelate $[Gd(trita)(H_2O)]^-$ as compared to the commercial contrast agent $[Gd(dota)(H_2O)]^-$, by replacing an ethylene by a propylene bridge in the ligand (see Scheme 1 for the ligands). This structural modification leads to an increase by two orders of magnitude in the water exchange rate, which falls into the optimal range to attain maximum proton relaxivities. In addition to the optimal water exchange rate, the stability of $[Gd(trita)(H_2O)]^-$ is sufficiently high to ensure safe medical use; this makes it a potential synthon for the development of high-relaxivity, macromolecular MRI contrast agents. In the present paper we demonstrate that the concept of increased steric crowding around the bound water site is not restricted to $[Gd(trita)(H_2O)]^-$ but is more general, and valid for linear chelates as well. It can be used generally to accelerate water exchange on nine-coordinate, monohydrated Gd^{III} chelates which undergo dissociative water exchange. In the family of linear ligands, we synthesized EPTPA-bz-NO_2^{5-}, $DPTPA^{5-}$ and DTTA-$prop^{5-}$ (Scheme 1). In comparison with the $DTPA^{5-}$, they all have the common feature of possessing one or two additional CH_2 moieties either in the backbone or in the carboxylic arm. Additionally, the bifunctional EPTPA-bz-NO_2^{5-} contains a nitrobenzyl unit which can easily be converted to a linker function in order to couple the chelate to macromolecules with a view to optimizing (slowing down) rotation. The macrocyclic ligand $TRITA^{4-}$ was first proposed by Maecke and co-workers for the complexation of radioactive metal ions, particularly In^{3+}, for radiopharmaceutical purposes.[10] This ligand was expected to ensure high thermodynamic and kinetic stability for the complex, and importantly, to have faster formation kinetics than DOTA-based chelators, which can be a problem in the preparation of radioactive chelates. Derivatives of the ligand $EPTPA^{5-}$ and their lanthanide complexes were reported recently in the literature.[11, 12] The DTTA-$prop^{5-}$ ligand was synthesized for the first time many years ago, and its lanthanide complexing abilities were investigated.[13] Our primary objective here was to show that all these ligands are similar with respect to water exchange on their Gd^{III} complexes: by tightly enveloping the metal ion they provoke an easier departure of the bound water in a dissociative exchange process.

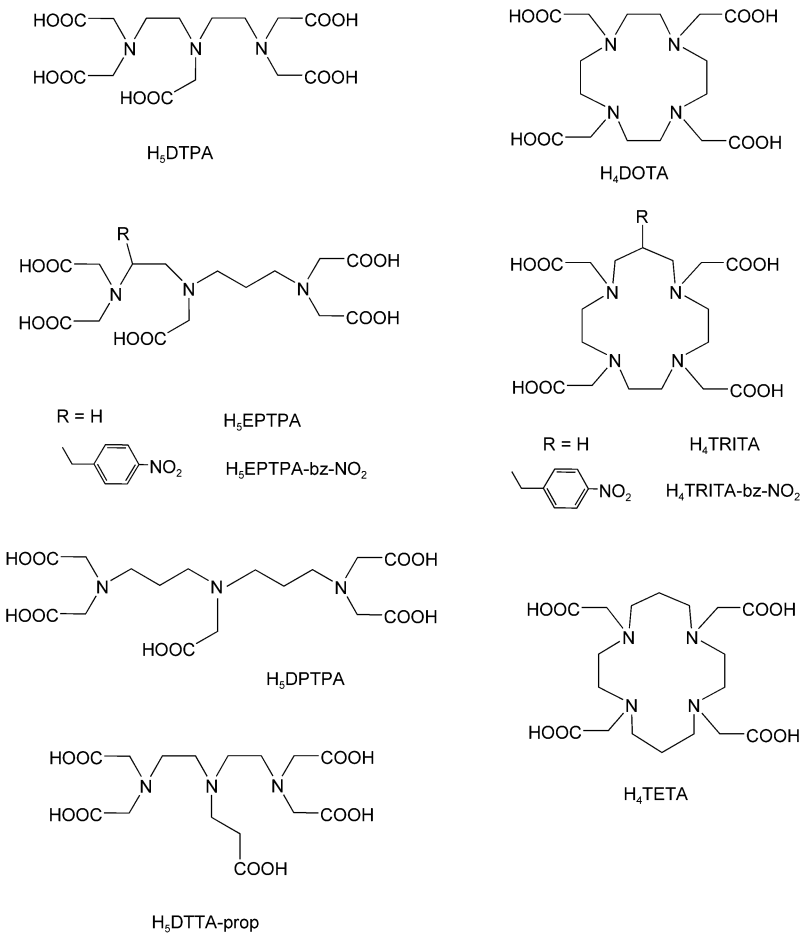

Scheme 1.

A sufficiently high thermodynamic stability of the Gd^{III} complex, and good selectivity of the ligand for Gd^{III} over other metal ions present in body fluids, are prerequisites for all biomedical applications. We have determined thermodynamic stability constants of several metal complexes involving Gd^{III} and some endogenously available metal ions such as Cu^{2+}, Zn^{2+} and Ca^{2+}, by pH potentiometry for the ligands EPTPA-bz-NO_2^{5-} and $DPTPA^{5-}$. Variable-temperature ^{17}O NMR spectroscopy was used to measure water exchange rates on the Gd^{III} complexes, and for $[Gd(eptpa\text{-}bz\text{-}NO_2)(H_2O)]^{2-}$ a combined ^{17}O NMR, EPR spectroscopy and variable-field proton relaxivity (NMRD) study resulted in parameters describing water exchange, rotation and electronic relaxation. Additionally, variable-pressure ^{17}O NMR measurements were carried out to determine the activation volume and thus to assess the water exchange mechanism on the linear $[Gd(eptpa)(H_2O)]^{2-}$ and the macrocyclic $[Gd(trita)(H_2O)]^{-}$ complexes. The results are discussed in the general context of designing high-efficacy contrast agents for magnetic resonance imaging.

Results and Discussion

Ligand protonation constants and stability constants of the metal complexes: The ligand protonation constants are defined as in Equation (1), and the stability constants of the metal chelates and the protonation constants of the complexes are expressed in Equation (2).

$$K_i = \frac{[H_iL]}{[H_{i-1}L]\,[H^+]} \quad (1)$$

$$K_{MH_iL} = \frac{[MH_iL]}{[MH_{i-1}L]\,[H^+]} \qquad i = 0, 1, 2 \quad (2)$$

The protonation constants of the ligands EPTPA-bz-NO_2^{5-} and $DPTPA^{5-}$ as well as the stability constants of their complexes formed with different metals (Gd^{III}, Zn^{II}, Ca^{II} and Cu^{II}) were determined by potentiometric titration (see Figure 1); the constants and the standard deviations are listed in Table 1.

In comparison with $DTPA^{5-}$, the ligands EPTPA-bz-NO_2^{5-} and $DPTPA^{5-}$ have a slightly higher protonation constant for the first protonation step, which occurs on the central nitrogen. A more important increase in the pK values of these ligands is observed for the second and third protonation steps. This effect is more pronounced for the dipropylenetriamine $DPTPA^{5-}$ than for the ethylenepropylene derivative EPTPA-bz-NO_2^{5-}: the pK_3 of $DPTPA^{5-}$ is three units higher than that of the diethylenetriamine $DTPA^{5-}$. Such an increase in the protonation constants with increasing chain length between the amino functions is usual for polyamines.[14] The second pK probably corresponds to the protonation of one of the terminal nitrogens which, as was shown for $DTPA^{5-}$ and $EPTPA^{5-}$ by ^1H NMR titration,[11, 15] induces the displacement of the first proton from the central to the other terminal nitrogen. This form, bearing the two protons on terminal nitrogens, is preferential as it is stabilized by internal hydrogen bridges between the protonated terminal nitrogens and the deprotonated carboxylates.

The thermodynamic stability constants for all the complexes were determined by direct potentiometry. The stability constant of $[Gd(eptpa)]^{2-}$, determined from a competition study with $EDTA^{4-}$, was found previously[11] to be similar to that for $[Gd(dtpa)]^{2-}$, that is, four orders of magnitude higher than the constant we obtained for $[Gd(eptpa\text{-}bz\text{-}NO_2)]^{2-}$. Recently, an even greater stability was reported for the Gd^{III} complex of the 4-benzyl derivative of EPTPA ($\log K_{GdL} = 23.79$).[16] Such high stability constants for Gd^{III} complexes of EPTPA and EPTPA derivative do not seem reasonable in comparison with the DTPA analogues, since the EPTPA complexes each have one six-membered chelate ring which is less stable than a five-membered ring. The low stability

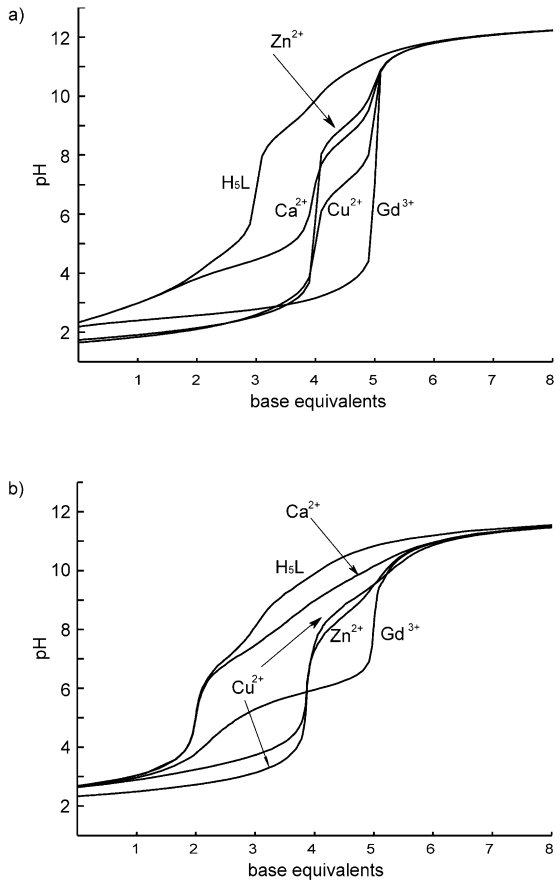

Figure 1. Potentiometric pH titration curves for the ligands a) EPTPA-bz-NO_2^{5-} and b) $DPTPA^{5-}$ in the absence and presence of Ca^{2+}, Zn^{2+}, Cu^{2+} or Gd^{3+} (metal/ligand ratio 1:1; $I = 0.1$ M $(CH_3)_4NCl$).

Table 1. Protonation and stability constants for the ligands and their metal complexes (25 °C; $I = 0.1$ M $(CH_3)_4NCl$).

	DTPA[a]	EPTPA-bz-NO_2	DPTPA	EPTPA[b]
pK_1	10.41	10.86 (±0.01)	10.91 (±0.01)	10.60
pK_2	8.37	8.91 (±0.02)	9.29 (±0.02)	8.92
pK_3	4.09	4.70 (±0.02)	7.07 (±0.01)	5.12
pK_4	2.51	3.25 (±0.02)	2.76 (±0.01)	2.80
pK_5	2.04	2.51 (±0.03)	2.19 (±0.03)	
$\log K_{GdL}$	22.50	19.20 (±0.02)	13.00 (±0.03)	22.77[c]
$\log K_{GdHL}$	1.80	3.40 (±0.02)	6.31 (±0.03)	
$\log K_{GdH_2L}$			5.42 (±0.06)	
$\log K_{ZnL}$	18.3	16.01 (±0.07)	15.60 (±0.03)	18.59
$\log K_{ZnHL}$	3.0	8.99 (±0.06)	8.06 (±0.04)	7.77
$\log K_{ZnH_2L}$		2.53 (±0.08)	3.17 (±0.06)	
$\log K_{CaL}$	10.89	9.38 (±0.04)	5.47 (±0.05)	14.45
$\log K_{CaHL}$	6.42	8.58 (±0.07)	9.53 (±0.06)	6.1
$\log K_{CaH_2L}$			7.9 (±0.1)	
$\log K_{CuL}$	21.45	18.47 (±0.04)	18.05 (±0.04)	19.31
$\log K_{CuHL}$	4.80	7.05 (±0.04)	8.90 (±0.04)	5.52
$\log K_{CuH_2L}$	2.96	2.80 (±0.04)	2.94 (±0.05)	

[a] Ref. [39]. [b] $I = 0.1$ M $(CH_3)_4NNO_3$, from ref. [11]. [c] For $[Gd(eptpa)]^{2-}$, we found $\log K_{GdL} = 18.75$ (±0.07) by direct titration and $\log K_{GdL} = 17.5$ (±0.3) by competition with EDTA (see text).

obtained for $[Gd(dptpa)]^{2-}$ clearly shows this tendency. The three-unit decrease in $\log K_{GdL}$ from L = DTPA to EPTPA-bz-NO_2 then the further stability decrease of six $\log K$ units for L = DPTPA seems more plausible. The species distribution curves obtained for $[Gd(eptpa\text{-}bz\text{-}NO_2)]^{2-}$ show that at the beginning of the titration (pH 2.32), 90% of all Gd^{3+} is free and the rest is in the form of the protonated complex. This makes possible a direct titration which usually results in more reliable stability constants than those obtained in competition studies. However, it is very unlikely that the nitrobenzyl unit has such an influence on the complex stability. Indeed, for the Y^{III} complexes formed with DTPA nitrobenzyl derivatives (the -bz-NO_2 group being on the carbon adjacent either to the central nitrogen or to a terminal one), the stability constants were similar to that for $[Gd(dtpa)]^{2-}$.[17] To rule out a strong effect of the nitrobenzyl function on the Gd^{III} complex stability, we also measured the stability constant for the parent complex $[Gd(eptpa)]^{2-}$ both by direct titration, as we did for $[Gd(eptpa\text{-}bz\text{-}NO_2)]^{2-}$ and by competition with $EDTA^{4-}$. The stability constants calculated were $\log K_{GdL} = 18.75 \pm 0.07$ from the direct titration and $\log K_{GdL} = 17.5 \pm 0.3$ from the competition method. The protonation constant of the complex ($\log K_{GdHL} = 4.1 \pm 0.1$) could be determined only from the direct titration. It is noteworthy that a similar progressive decrease of the stability was observed in the family of macrocyclic chelates from the 12-membered macrocyclic $[Gd(dota)]^-$ to the 13-membered $[Gd(trita)]^-$ and the 14-membered $[Gd(teta)]^-$ ($\log K_{GdL} = 24.0$, 19.2 and 13.8 for L = DOTA, TRITA and TETA, respectively).[18] Whereas for DOTA all chelate rings formed upon metal complexation are five-membered, for TRITA there is one and for TETA there are two six-membered (and thus less stable) chelate rings, which is reflected well in the decreasing order of stability. It is interesting that between $[Gd(eptpa)]^{2-}$ and $[Gd(dptpa)]^{2-}$, as well as between $[Gd(trita)]^-$ and $[Gd(teta)]^-$, the hydration state of the metal changes from $q = 1$ to $q = 0$ ($[Gd(eptpa)(H_2O)]^{2-}$; $[Gd(trita)(H_2O)]^-$; $[Gd(dptpa)]^{2-}$; $[Gd(teta)]^-$) as a consequence of a better wrapping up of the metal ion by the larger $DPTPA^{5-}$ and $TETA^{4-}$ (discussed below). Thus, one could reason that such a good enveloping of the metal would increase the stability of the complex. A complex with an inner-sphere water might be more readily susceptible to an outside attack and this susceptibility would consequently decrease its stability. However, the example of both the linear and the macrocyclic complexes shows that the stability difference between the five- and six-membered chelate rings formed on complexation is more important than the effect of a better enveloping by the ligand.

The thermodynamic stability constant reported for $[Gd(dtta\text{-}prop)]^{2-}$ ($\log K_{GdL} = 16.7$)[13] is also lower than that of $[Gd(dtpa)]^{2-}$. Again, the attenuation is explained by the higher stability of a five-membered chelate ring formed with acetates upon metal chelation than with a six-membered chelate ring formed with the propionate function. Curiously, the decrease in complex stability is smaller when the propionate arm is on a terminal nitrogen. For the Gd^{III} complex of the DTPA derivative containing one propionate in a terminal position a stability constant of $\log K_{GdL} = 19.7$ has been reported.[19]

The thermodynamic stability constants alone are not sufficient to compare different complex stabilities under physiological conditions. The conditional stability constants, or more frequently the pM values are considered to be a

better gauge of physiologically relevant complex stability. The p*M* values reflect the influence of the ligand basicity and the protonation of the complex. The higher the p*M*, the more stable is the complex under the given conditions. p*M* values for several Gd^{III} complexes are compared in Table 2.

Table 2. p*M* values of Gd^{III} complexes under physiologically relevant conditions (pH 7.4; $[Gd]_{total} = 1\,\mu M$; $[L]_{total} = 10\,\mu M$).

Ligand	pGd
DTPA[a]	19.1
DTPA-BMA[b]	15.8
EPTPA	14.7
EPTPA-bz-NO_2	15.3
DTTA-prop[c]	14.9
DOTA[d]	19.2
TRITA[d]	14.6

For the protonation constants of the ligand and the stability constant of the Gd^{III} complex see [a] ref. [39]. [b] Ref. [40]. [c] Ref. [13]. [d] Ref. [18].

In an MRI examination, upon injection into the bloodstream the Gd^{III} complex enters a very complex system from the coordination chemistry point of view. The free metal ion and the free ligand—if dissociation of the complex occurs—or the complex itself can participate in many side reactions. Besides the protonation of the free ligand and the complex, which is taken into account in the p*M* values, competition between Gd^{3+} and endogenous metal ions (most importantly Ca^{2+}, Zn^{2+} and Cu^{2+}) has also to be considered. The conditional stability constants calculated by considering all these equilibria were indeed found to correlate with experimental LD_{50} values.[20] This illustrates the importance of selectivity of the ligand for Gd^{3+} over endogenous metals, particularly Zn^{2+} since its concentration is the greatest. The stability of the EPTPA-bz-NO_2 complexes with the endogenously available metal ions, similarly to Gd^{III}, is lower than that of the corresponding DTPA chelates. Overall, the selectivity of EPTPA-bz-NO_2^{5-} for Gd^{3+} over these metal ions (defined as $\log(K_{GdL}/K_{ML})$ with $M = Zn^{2+}$, Cu^{2+} or Ca^{2+}) is not very different from that of $DTPA^{5-}$. For the Zn^{II}–, Cu^{II}– and Ca^{II}–EPTPA chelates, higher stability constants were previously reported than our values determined for the EPTPA-bz-NO_2 analogues, the largest difference being in the Ca^{II} complex stabilities.[11] Recently, for the Ca^{II}–bz-EPTPA complex a stability constant ($\log K_{CaL} = 16.0$) five orders of magnitude higher than that of $[Cadtpa]^{3-}$ was obtained.[16] Such high stability seems unlikely. For $DPTPA^{5-}$, the stability of all metal complexes studied is considerably lower than that of the DTPA chelates. In comparison with EPTPA-bz-NO_2^{5-}, there is a large decrease in stability for Gd^{III} and Ca^{II}, whereas the Cu^{II} and Zn^{II} complex stabilities do not differ much for the two ligands. In general, the DPTPA chelates have a stronger tendency to form protonated complexes.

UV/Vis study: To learn about the hydration state of the EPTPA-bz-NO_2–lanthanide(III) complexes, we performed a variable-temperature UV/Vis study on an aqueous solution of the Eu^{III} analogue. The $^7F_0 - {}^5D_0$ transition band of Eu^{III} (577.5–581.5 nm) is very sensitive to the coordination environment and is often used to test the presence of differently coordinated species.[21] $[Eu(eptpa\text{-}bz\text{-}NO_2)(H_2O)]^{2-}$ has a single, temperature-invariant absorption band in this region, which proves the absence of a hydration equilibrium in solution within the temperature range studied (25–68 °C). By analogy, we assume that the same hydration mode, and thus no hydration equilibrium, exists for the corresponding Gd^{III} complex as well.

^{17}O NMR, EPR spectroscopy and NMRD measurements: The water exchange rate was determined for the Gd^{III} complexes of the ligands EPTPA-bz-NO_2^{5-}, $EPTPA^{5-}$ and $DTTA\text{-}prop^{5-}$ from a variable-temperature ^{17}O NMR study. Additionally, EPR spectra were recorded for aqueous solutions of $[Gd(eptpa\text{-}bz\text{-}NO_2)(H_2O)]^{2-}$, $[Gd(eptpa)(H_2O)]^{2-}$ and $[Gd(dptpa)]^{2-}$ and variable-temperature proton relaxation rates were measured on $[Gd(eptpa\text{-}bz\text{-}NO_2)(H_2O)]^{2-}$ with the objective of determining parameters that describe water exchange, rotation, electronic relaxation and proton relaxivity.

All available experimental data for a given Gd^{III} complex, that is, the ^{17}O NMR chemical shifts ($\Delta\omega_r$), longitudinal ($1/T_{1r}$) and transverse ($1/T_{2r}$) relaxation rates, the electronic relaxation rates ($1/T_{2e}$) and the longitudinal proton relaxivities (r_1, when measured) were analyzed simultaneously (for the equations used in the data analysis, see the Appendix). For $[Gd(dptpa)]^{2-}$, the $1/T_{1r}$ and $1/T_{2r}$ values are equal within the experimental error and the $\Delta\omega_r$ values are about 10 % of those generally measured for monohydrated Gd^{III} complexes, indicating only an outer-sphere contribution to the chemical shift. This proves that $[Gd(dptpa)]^{2-}$ contains no inner-sphere water molecule. The NMRD profile is also in accordance with a pure outer-sphere effect. We assumed that $[Gd(eptpa\text{-}bz\text{-}NO_2)(H_2O)]^{2-}$, $[Gd(eptpa)(H_2O)]^{2-}$ and $[Gd(dtta\text{-}prop)(H_2O)]^{2-}$ each had one inner-sphere water molecule. The scalar coupling constants thus obtained for these complexes are in the usual range for coupling constants of Gd^{III} complexes, which justifies the assumption of $q = 1$. Furthermore, on the basis of the UV/Vis study discussed above, we could exclude any coordination/hydration equilibrium for $[Eu(eptpa\text{-}bz\text{-}NO_2)(H_2O)]^{2-}$. The experimental ^{17}O NMR, NMRD and EPR data and the fitted curves for $[Gd(eptpa\text{-}bz\text{-}NO_2)(H_2O)]^{2-}$ are presented in Figure 2 whereas for $[Gd(dptpa)]^{2-}$, $[Gd(eptpa)(H_2O)]^{2-}$ and $[Gd(dtta\text{-}prop)(H_2O)]^{2-}$ they are given in the Supporting Information. All parameters obtained in the fit are shown in Table 3.

Recent studies on the rotation of small Gd^{III} chelates showed that internal motions of the coordinated water molecule had to be taken into account.[22, 23] Therefore, in the simultaneous analysis of ^{17}O NMR, EPR and NMRD data for $[Gd(eptpa\text{-}bz\text{-}NO_2)(H_2O)]^{2-}$ we separated the rotational correlation time of the $Gd-O_{water}$ vector, τ_{RO}, influencing longitudinal ^{17}O relaxation, and the rotational correlation time of the $Gd-H_{water}$ vector, τ_{RH}, influencing ^1H relaxivities [Eqs. (A7) and (A19)]. For the ratio of the rotational correlation time of the $Gd-H_{water}$ and $Gd-O_{water}$ vectors, τ_{RH}/τ_{RO}, similar values have been found for different Gd^{III} complexes, both by experimental studies and MD simulations ($\tau_{RH}/\tau_{RO} = 0.65 \pm 0.2$).[22, 23] This τ_{RH}/τ_{RO} ratio, within the given

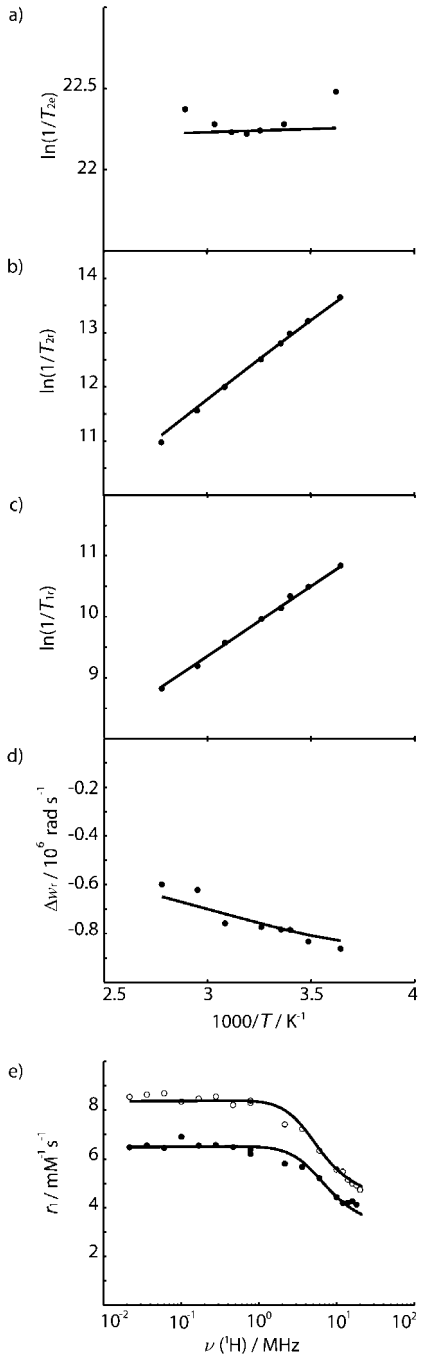

Figure 2. Temperature dependence of a) transverse electronic relaxation rates at $B = 0.34$ T; b) transverse and c) longitudinal ^{17}O relaxation rates; d) ^{17}O chemical shifts at $B = 9.4$ T; and e) ^{1}H NMRD profiles at 25 °C (○) and 37 °C (●) for $[Gd(eptpa\text{-}bz\text{-}NO_2)(H_2O)]^{2-}$. The lines represent curves fitted to the experimental points.

error, can be considered as a general value for the ratio of the two rotational correlation times. Hence, in the analysis of ^{17}O NMR and NMRD data for $[Gd(eptpa\text{-}bz\text{-}NO_2)(H_2O)]^{2-}$, we fixed this ratio at 0.65 and fitted τ_{RO}, considered as a real rotational correlation time of the complex. The quadrupolar coupling constant for the bound water oxygen, $(\chi(1+(\eta^2/3))^{1/2}$, was also fitted for $[Gd(eptpa\text{-}bz\text{-}NO_2)(H_2O)]^{2-}$: a slightly higher value, 10.1 MHz, was found than that for pure water ($(\chi(1+(\eta^2/3))^{1/2} = 7.58$ MHz). To compare the three Gd^{III} complexes studied here, the same value of the quadrupolar coupling constant was then used in the analysis of ^{17}O longitudinal relaxation rates for $[Gd(eptpa)(H_2O)]^{2-}$ and $[Gd(dtta\text{-}prop)(H_2O)]^{2-}$. The r_{GdO} and r_{GdH} distances were fixed at 2.50 and 3.10 Å, respectively. The rotational correlation times obtained for $[Gd(eptpa\text{-}bz\text{-}NO_2)(H_2O)]^{2-}$ from the simultaneous analysis, and for $[Gd(eptpa)(H_2O)]^{2-}$ and $[Gd(dtta\text{-}prop)(H_2O)]^{2-}$ from longitudinal ^{17}O relaxation rates, are reasonable and they are typical of low molecular weight chelates.

Table 3. Parameters obtained for $[GdL(H_2O)]^{2-}$ chelates from the analysis of ^{17}O NMR, NMRD and EPR data.

Ligand	EPTPA-bz-NO_2^{5-}	$EPTPA^{5-}$ [a]	DTTA-$prop^{5-}$ [b]
k_{ex}^{298} [10^8 s^{-1}]	1.5 ± 0.4	3.3 ± 0.4	0.31 ± 0.1
ΔH^{+} [kJ mol^{-1}]	22.1 ± 1.8	27.9 ± 1.1	30.8 ± 2.0
ΔS^{+} [J mol^{-1} K^{-1}]	-9.1 ± 5.0	$+11.0 \pm 3.0$	$+2.0 \pm 5.0$
ΔV^{+} [cm^3 mol^{-1}]		$+6.6 \pm 0.3$	
$A/\hbar$ [10^6 rad s^{-1}]	-3.2 ± 0.2 [c]	-3.9 ± 0.2 [c]	-3.3 ± 0.3 [c]
τ_{rO}^{298} [ps]	122 ± 12	75 ± 6	121 ± 10
E_R [kJ mol^{-1}]	19.0 ± 1.7	17.7 ± 1.0	17.4 ± 2.3
τ_V^{298} [ps]	22 ± 1	22.4 ± 1.1	18 ± 2
E_v [kJ mol^{-1}] [d]	*1*	*1*	*1*
Δ^2 [10^{20} s^{-2}]	0.4 ± 0.3	0.76 ± 0.2	1.2 ± 0.2
D_{GdH}^{298} [10^{-10} m^2 s^{-1}]	29.7 ± 2.2		
E_{DGdH} [kJ mol^{-1}]	27.5 ± 2.9		

[a] From ^{17}O NMR and EPR data. [b] Only from ^{17}O transverse and longitudinal relaxation rates and chemical shifts. [c] The empirical constant for the outer-sphere contribution to the chemical shift was fixed at $C_{os} = 0.1$. [d] Italic values fixed in the fit.

Over the whole temperature range and for all the Gd^{III} complexes studied, the transverse ^{17}O relaxation rates $1/T_{2r}$ decrease with increasing temperature, indicating that these systems are in the fast exchange regime. $1/T_{2r}$ is thus determined by the relaxation rate of the coordinated water molecule $1/T_{2m}$, which itself is influenced by the water residence time $\tau_m = 1/k_{ex}$, the longitudinal electronic relaxation rate $1/T_{1e}$ and the nuclear hyperfine coupling constant $A/\hbar$ [Eq. (A9)]. The transverse relaxation rates $1/T_{2e}$ can be measured experimentally by EPR, whereas the longitudinal relaxation rates $1/T_{1e}$ are calculated from the $1/T_{2e}$ values through Equations (A12) – (A14). The NMRD data also contain information on electronic relaxation. For $[Gd(eptpa)(H_2O)]^{2-}$, variable-temperature EPR spectra were recorded at $B = 8.1$ T (225 GHz), in order to obtain direct information on the electron spin relaxation. EPR measurements at such high frequency are particularly useful since this magnetic field is close to that of the ^{17}O NMR study (9.4 T). Therefore the problems associated with the inappropriate theory used to calculate electronic relaxation rates at high field (necessary for the analysis of the ^{17}O relaxation rates) from the EPR data measured at much lower frequency (usually at the X band, $B = 0.34$ T) can be minimized. The recently developed Rast – Borel theory, involving both transient and static zero field splitting, has contributed much to the understanding of electron spin relaxation of Gd^{III} complexes.[24] It results in physically meaningful parameters to describe electron spin relaxation and it allowed an improved combined fit of variable-field ^{17}O, ^{1}H and electronic relaxation rates.[25] However, this profound analysis can be applied only when EPR data are available for a wide range of

magnetic fields. Therefore, in the absence of variable-field EPR spectra, the experimental data for all three systems were analyzed according to the traditional Solomon–Bloembergen–Morgan theory. Here only a transient zero-field-splitting mechanism (ZFS) is considered which is characterized by the trace of the square of the zero-field-splitting tensor (Δ^2) and the correlation time for the modulation of the ZFS (τ_v) as fitted parameters.[26] However, one has to be aware of the shortcomings of this simplified theory and the resulting parameters, which have no real physical meaning but are only fitting parameters,[27] must not be overinterpreted.

The pressure dependence of the transverse ^{17}O relaxation rates gives access to the water exchange mechanism. Transverse ^{17}O relaxation rates, $1/T_{2r}$, were measured at $B = 9.4$ T and two different temperatures for $[Gd(eptpa)(H_2O)]^{2-}$ and $[Gd(trita)(H_2O)]^{-}$. The latter can be considered as the macrocyclic analogue of $[Gd(eptpa)(H_2O)]^{2-}$, since $TRITA^{4-}$ is obtained by substituting one ethylene by a propylene bridge in the ligand $DOTA^{4-}$ (Scheme 1). We have shown recently that the water exchange on this macrocyclic Gd^{III} complex is remarkably faster than on $[Gd(dota)(H_2O)]^{-}$.[9] At the temperatures and magnetic field used in the variable-pressure study, $1/T_{2r}$ is at the fast exchange limit and is dominated by the scalar interaction. For $[Gd(eptpa)(H_2O)]^{2-}$, the increase in $1/T_{2r}$ with pressure is therefore due to the slowing down of the water exchange process and suggests a dissociative interchange (I_d) mechanism.[28] For $[Gd(trita)(H_2O)]^{-}$, the $1/T_{2r}$ values are practically independent of pressure at both temperatures, pointing to an interchange mechanism. The scalar coupling constant ($A/\hbar$) was previously found to be independent of pressure,[29] so we assume that it is constant and equal to the value in Table 3. τ_v was also assumed to be independent of pressure. In fact, ascribing to τ_v a pressure dependence equivalent to activation volumes between -4 and $+4\ cm^3 mol^{-1}$ had a negligible effect on the fitted $\Delta V^{\neq}$ value. The experimental data points and the results of the least-squares fits for $[Gd(eptpa)(H_2O)]^{2-}$ and $[Gd(trita)(H_2O)]^{-}$ are shown in Figure 3. The fitted parameters are $\Delta V^{\neq} = (+6.6 \pm 0.3)\ cm^3 mol^{-1}$, $(k_{ex})_0^{293} = (2.9 \pm 0.1) \times 10^8\ s^{-1}$ and $(k_{ex})_0^{323} = (1.1 \pm 0.1) \times 10^9\ s^{-1}$ for $[Gd(eptpa)(H_2O)]^{2-}$ and $\Delta V^{\neq} = (-1.5 \pm 1.0)\ cm^3 mol^{-1}$, $(k_{ex})_0^{323} = (2.7 \pm 0.1) \times 10^8\ s^{-1}$ and $(k_{ex})_0^{323} = (5.0 \pm 0.1) \times 10^8\ s^{-1}$ for $[Gd(trita)(H_2O)]^{-}$. (The error on $\Delta V^{\neq}$ is usually considered to be $\pm 1\ cm^3 mol^{-1}$ or 10% of the $\Delta V^{\neq}$ value, whichever is the larger, to take into account possible effects of non-random errors.)

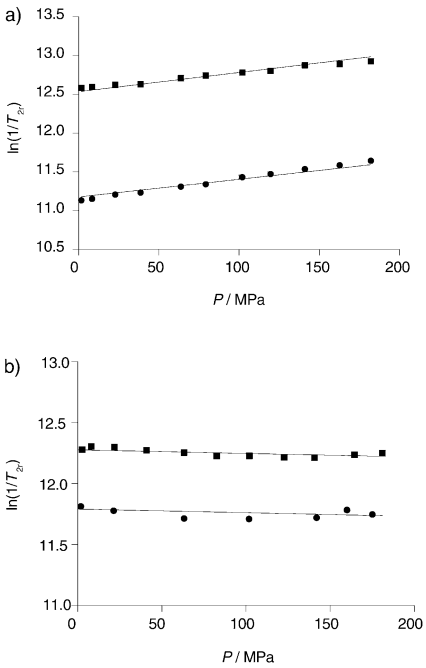

Figure 3. Pressure dependence of the reduced transverse ^{17}O relaxation rates at $B = 9.4$ T for a) $[Gd(eptpa)(H_2O)]^{2-}$ at 20 °C (squares) and 50 °C (circles) and b) for $[Gd(trita)(H_2O)]^{-}$ at 26 °C (squares) and 50 °C (circles).

Water exchange: The objective of this study was to prove that an increased steric compression around the water binding site in nine-coordinated, monohydrated Gd^{III} complexes that undergo dissociative water exchange results in an increased water exchange rate. Since all Gd^{III} complexes currently applied as MRI contrast agents belong to this class of chelates, and since slow water exchange represents an important drawback for the new generation (macromolecular) contrast agents, the results of such a study will have important implications for further research in the field. We modified the most commonly used ligands, $DTPA^{5-}$ and $DOTA^{4-}$, to induce more steric crowding in the Gd^{III} complex without much sacrificing the high thermodynamic complex stability. The parameters describing water exchange for the parent $[Gd(dota)(H_2O)]^{-}$ and $[Gd(dtpa)(H_2O)]^{2-}$ and for the Gd^{III} complexes of the derivative ligands with elongated amine backbones are compared in Table 4. The water exchange rate on $[Gd(eptpa)(H_2O)]^{2-}$, $[Gd(eptpa\text{-}bz\text{-}NO_2)(H_2O)]^{2-}$, $[Gd(trita)(H_2O)]^{-}$ and $[Gd(trita\text{-}bz\text{-}NO_2)(H_2O)]^{-}$ is almost two orders of magnitude higher than on the DTPA or DOTA complex. The rate we obtained for $[Gd(eptpa)(H_2O)]^{2-}$ is

Table 4. Comparison of water exchange parameters for $[GdL(H_2O)]$ chelates.

Complex	k_{ex}^{298} [$10^6\ s^{-1}$]	$\Delta H^{\neq}$ [$kJ\ mol^{-1}$]	$\Delta S^{\neq}$ [$J\ mol^{-1}\ K^{-1}$]	$\Delta V^{\neq}$ [$cm^3\ mol^{-1}$]	Ref.
$Gd(H_2O)_8^{3+}$	804	15.3	−23	−3.3	[41]
$[Gd(dtpa)(H_2O)]^{2-}$	3.3	51.6	+53	+12.5	[41]
$[Gd(eptpa)(H_2O)]^{2-}$	330	27.7	+11	+6.6	this work
$[Gd(eptpa\text{-}bz\text{-}NO_2)(H_2O)]^{2-}$	150	22.1	−9		this work
$[Gd(dtta\text{-}prop)(H_2O)]^{2-}$	31	30.8	+2		this work
$[Gd(dota)(H_2O)]^{-}$	4.1	49.8	+49	+10.5	[41]
$[Gd(trita)(H_2O)]^{-}$	270	17.5	−24	−1.5	[9], this work
$[Gd(trita\text{-}bz\text{-}NO_2)(H_2O)]^{-}$	120	35.5	+20		[9]

even higher than the value previously reported ($k_{ex}^{298} = 94 \times 10^6\ s^{-1}$).[12] These results confirm the expectations that an additional methylene group in the amine backbone of the ligand leads to a better wrapping-up of the metal by the chelator, leaving less space for the inner-sphere water. In the case of $[Gd(trita)(H_2O)]^-$, this could be nicely related to the crystal structure.[9] As a proof of the compressed structure around the bound water site, the $O_{carboxylate}$-Gd-$O_{carboxylate}$ angles are much smaller in $[Gd(trita)(H_2O)]^-$ than in $[Gd(dota)(H_2O)]^-$ (136.7 and 142.7 versus 146°).[9, 30] Another consequence of the steric compression is the remarkably long distance between the plane of the carboxylate oxygen atoms and the metal, 0.83 Å in $[Gd(trita)(H_2O)]^-$ versus 0.70 Å in $[Gd(dota)(H_2O)]^-$. Since the Gd-bound water–oxygen distance is similar in the two complexes (2.48 Å in TRITA, and 2.45 Å in DOTA), the final result is that the bound water molecule in $[Gd(trita)(H_2O)]^-$ is much closer to the negatively charged carboxylates; this also facilitates its departure. It would be interesting to compare the X-ray structures of the linear $[Gd(dtpa)(H_2O)]^{2-}$, $[Gd(eptpa)(H_2O)]^{2-}$ and $[Gd(dptpa)]^{2-}$ complexes as well, but so far we have failed to obtain suitable crystals of the last two compounds.

Theoretical calculations based on the Solomon–Bloembergen–Morgan theory of paramagnetic relaxation show that the optimal water exchange rates to attain the highest proton relaxivities, and so the highest efficacy for Gd^{III}-based contrast agents, are around $k_{ex} = 10^8\ s^{-1}$. Thus the $EPTPA^{5-}$ and $TRITA^{4-}$ chelates ensure the optimal exchange rate. In addition, the Gd^{III} complexes have a sufficiently high thermodynamic stability for these ligands to be potential building blocks for the construction of slowly tumbling, high molecular weight MRI contrast agents.

It is interesting that in terms of hydration of the Gd^{III} complexes, the linear "DTPA" and the macrocyclic "DOTA" family behave in a similar way. When the amine backbone is extended by one methylene group ($EPTPA^{5-}$ and $TRITA^{4-}$) the monohydrated structure (without a hydration equilibrium) is retained in the Gd^{III} complex of both ligands, whereas the addition of a second CH_2 results in the elimination of the water molecule from the inner coordination sphere ($DPTPA^{5-}$ and $TETA^{4-}$). As mentioned above, the analogy is also valid for the decreasing thermodynamic stability of the respective Gd^{III} complexes.

The variable-pressure ^{17}O NMR measurements for $[Gd(eptpa)(H_2O)]^{2-}$ and $[Gd(trita)(H_2O)]^-$ gave the activation volume of water exchange. The value for $[Gd(eptpa)(H_2O)]^{2-}$ ($\Delta V^{\neq} = +6.6 \pm 1.0\ cm^3\,mol^{-1}$) is, as expected, in agreement with a dissociative interchange mechanism, though with considerably less dissociative character than was found for $[Gd(dtpa)(H_2O)]^{2-}$ ($\Delta V^{\neq} = +12.5\ cm^3\,mol^{-1}$; limiting dissociative (D) mechanism). The activation volume obtained for $[Gd(trita)(H_2O)]^-$ ($\Delta V^{\neq} = -1.5 \pm 1.0\ cm^3\,mol^{-1}$) shows an interchange mechanism, however. The less positive activation entropy and the lower activation enthalpy also point to a less dissociative exchange than for $[Gd(dota)(H_2O)]^-$. Thus, there is strong participation of the incoming water in the rate-determining step which, in addition to the repulsive effect arising from the proximity of the carboxylates to the inner-sphere water, contributes to the increased rate of water exchange.

The ligand $(DTTA\text{-}prop)^{5-}$ has a propionate function substituted for the central acetate of $DTPA^{5-}$ and thus contains an additional methylene group in one of the coordinating arms instead of the ligand backbone. The water exchange on $[Gd(dtta\text{-}prop)(H_2O)]^{2-}$ is one order of magnitude faster than on $[Gd(dtpa)(H_2O)]^{2-}$, but still one order of magnitude lower than on $[Gd(eptpa)(H_2O)]^{2-}$. This seems to show that the elongation of the backbone is much more important than the elongation of a coordinating arm to induction of steric crowding around the water bonding site. This is plausible since a propionate arm is much more flexible than the backbone which, overall, is coordinated to the metal at three points through the three amine groups.

Conclusion

On the basis of structural considerations in the inner sphere of linear and macrocyclic Gd^{III} complexes, we succeeded in accelerating water exchange by inducing steric compression around the water bonding site. The increased steric crowding was achieved by replacing an ethylene bridge of $DOTA^{4-}$ or $DTPA^{5-}$ by a propylene bridge, or by replacing one acetate by a propionate coordinating group. Although this modification reduces the thermodynamic stability of the chelate slightly, the Gd^{III} complexes are stable enough to be used in medical diagnostics as MRI contrast agents. Therefore these chelates are potential building blocks for the development of high-relaxivity macromolecular agents.

Experimental

Synthesis of the ligands: All reagents used for the synthesis of the ligands were purchased from commercial sources unless otherwise noted. H_4TRITA used for the variable-pressure ^{17}O NMR study was prepared as described previously.[9]

Methyl DL-*p*-nitrophenylalanate (1): DL-*p*-Nitrophenylalanine (10.0 g, 48 mmol) was placed in a three-necked flask (250 mL) equipped with a gas inlet, a thermometer and a $CaCl_2$ drying tube. The flask was purged with dry argon and CH_3OH (125 mL) was introduced. Anhydrous HCl gas was bubbled into the stirred suspension to dissolve the DL-*p*-nitrophenylalanine; after 10 min all of it had dissolved and the solution was yellow. The mixture was cooled to 10 °C. After 30 min of bubbling in the HCl, the yellow solution became cloudy. The solution was saturated with HCl gas 90 min after the beginning of the precipitation. Stirring at 10 °C was then continued for another 30 min. To complete the precipitation the flask was kept at −4 °C overnight and at −20 °C for 24 h. The white crystals were filtered and dried under reduced pressure to give **1** (9.79 g, 92 %). ^1H NMR (200 MHz, D_2O [HDO 4.80 ppm]): $\delta = 3.2–3.4$ (m, 8H), 3.69 (s, 3H), 4.38 (t, $J = 7.2$ Hz, 1H), 7.39 (d, $J = 7.9$ Hz, 2H), 8.12 (d, $J = 7.9$ Hz, 2H).

DL-*p*-Nitrophenylalanate *N*-(3-aminopropyl) amide (2): 1,3-Diaminopropane (30.3 g, 408 mmol) was added under argon to a three-necked flask (250 mL) equipped with a gas inlet, a $CaCl_2$ drying tube and a gas outlet. When ester **1** (7.81 g, 35 mmol) was added over a 3 h period, the clear solution immediately turned dark red. The solution was stirred for 24 h at room temperature and then concentrated in a rotary evaporator to a dark red viscous oil. Aqueous NH_3 (25 %; 55 mL) was added to this solution and the pH was adjusted to 11.6 with NaOH (50 %; 0.5 mL). The aqueous phase was extracted with CH_2Cl_2 (10 portions of 55 mL). The organic extracts were pooled, dried with Na_2SO_4, filtered, concentrated and dried under reduced pressure to give **2** as an amorphous brown powder (6.69 g, 72 %).

^{1}H NMR (200 MHz, $CDCl_3$ [$CHCl_3$ 7.30 ppm]): $\delta = 1.51$ (m, 2H), 2.74 (t, $J = 6.5$ Hz, 2H), 2.92 (dd, $J = 13.8$ Hz, 8.4 Hz, 1H), 3.27–3.42 (m, 3H), 3.65 (dd, $J = 8.6$ Hz, 4.3 Hz, 1H), 7.40 (d, $J = 8.5$ Hz, 2H), 7.51 (br s, 1H), 8.18 (d, $J = 8.5$ Hz, 2H).

(*p*-Nitrobenzyl)ethylenepropylenetriamine (3): Amide **2** (6.0 g, 22.5 mmol) was placed under argon in a three-necked flask (1 L) equipped with a condenser, a septum and an addition funnel. Anhydrous THF (180 mL) was purged with argon, then cannulated into the addition funnel and added in one portion. The amide dissolved only partially. The solution was kept at 0 °C while BH_3/THF (1M; 180 mL) was cannulated into the addition funnel and added dropwise over a 30 min period, after which all the amide had dissolved. The solution was warmed gradually, brought to reflux for 10 h, kept for 7 h at room temperature, then cooled to 5 °C with an ice bath. The excess of borane was quenched by addition of cold water (13 mL). The mixture was concentrated under reduced pressure to give a brown oil. HCl (6M; 130 mL) was added to the oil, and the resulting solution was heated under reflux for 3 h. The mixture was evaporated to dryness and the remaining yellow residue was dissolved in H_2O (90 mL) and aqueous NH_3 (25%; 90 mL). The pH was adjusted to 12 with KOH (5M). This solution was extracted with CH_2Cl_2 (10 portions of 100 mL). The organic extracts were pooled, dried with Na_2SO_4, filtered, concentrated and dried under reduced pressure to give **3** as a yellow oil (5.20 g, 92%). ^{1}H NMR (200 MHz, $CDCl_3$ [$CHCl_3$ 7.30 ppm]): $\delta = 1.63$ (m, 2H), 2.46 (dd, $J =$ 11.6 Hz, 8.3 Hz, 1H), 2.6–3.0 (m, 7H), 3.13 (m, 1H), 7.36 (d, $J = 8.4$ Hz, 2H), 8.15 (d, $J = 8.4$ Hz, 2H).

(*p*-Nitrobenzyl)ethylenepropylenetriaminepentaacetic acid penta-*tert*-butyl ester (4): Amine **3** (5.2 g, 20.6 mmol) was added under argon to a three-necked flask (500 mL) equipped with a gas inlet, an addition funnel and a $CaCl_2$ drying tube. Anhydrous DMF (170 mL) was added in one portion. After the dissolution of **3**, DIEA (43 mL, 247 mmol) was added in one portion. *tert*-Butyl bromoacetate (27.5 mL, 157 mmol) was added, whereupon the solution turned brown. When KI (3.8 g, 23 mmol) was added in one portion the solution became orange and warm to the touch. The mixture was stirred under argon at room temperature for 18 h. Evaporation of the solvent under reduced pressure gave a brown solid together with a white solid. The residue was partitioned between Et_2O (270 mL) and H_2O (100 mL). The organic phase was washed with H_2O (two 130 mL portions) and with a saturated NaCl solution (two 70 mL portions), dried with Na_2SO_4, filtered and evaporated to dryness. The crude product **4** was purified on a silica gel column (3.0 cm × 20 cm) using ethyl acetate/heptane (3:1 *v*/*v*) as eluent to give **4** as a light yellow oil (7.2 g, 42%). $R_f = 0.65$ (ethyl acetate/heptane 3:1); ^{1}H NMR (200 MHz, $CDCl_3$ [$CHCl_3$ 7.30 ppm]): $\delta =$ 1.40–1.48 (m, 45H), 1.58 (m, 2H), 2.42 (dd, $J = 13.1$, 8.2 Hz, 1H), 2.54–3.15 (m, 8H), 3.23 (s, 2H), 3.39 (s, 8H), 7.49 (d, $J = 8.8$ Hz, 2H), 8.11 (d, $J =$ 8.8 Hz, 2H).

(*p*-Nitrobenzyl)ethylenepropylenetriaminepentaacetic acid (H_5EPTPA-bz-NO_2; 5): Ester **4** (4.27 g, 5.2 mmol) and HCl (6M; 200 mL) were heated under reflux for 14 h and then kept at room temperature for 12 h. The reaction solution was washed with ethyl acetate (five 200 mL portions). Evaporation of the aqueous phase gave a slightly yellow powder. The product was recrystallized twice from EtOH/Et_2O to give **5** as white crystals (565 mg, 20%). ^{1}H NMR (200 MHz, D_2O [HDO 4.80 ppm]): $\delta = 2.24$ (m, 2H), 2.85 (dd, $J = 7.6$ Hz, 13.4 Hz, 1H), 3.10–3.90 (m, 8H), 3.70 (s, 6H), 4.05 (s, 4H), 7.52 (d, $J = 8.7$ Hz, 2H), 8.23 (d, $J = 8.7$ Hz, 2H); MS (ESI): m/z: 543.2 $[M+H]^+$; elemental analysis calcd (%) for $C_{22}H_{30}N_4O_{12}\cdot H_2O$ (560.5): C 47.14, H 5.75, N 10.00; found: C 47.30, H 6.13, N 9.80.

Dipropylenetriaminepentaacetic acid (H_5DPTPA; 6): NaOH solution (12.3M, 46 mL, 570 mmol) was added dropwise to a solution of monochloroacetic acid (27 g, 290 mmol) in H_2O (14 mL) cooled with an ice bath at 5 °C. Bis(3-aminopropyl)amine (5.4 mL, 38 mmol) was added to the reaction solution. The ice bath was removed and the temperature rose to 50 °C in 1 h. The solution was stirred at room temperature for 18 h. The mixture was cooled to 5 °C and H_2SO_4 (95%, 10 mL) was added dropwise to adjust the pH to approximately 1.5. Evaporation of the solvent gave a white solid (30 g). A portion of the crude product **6** (15 g) was loaded onto a cation-exchange column (Dowex 50WX2, 200–400 mesh, H^+ form, 100 g) and washed with H_2O (700 mL). The crude product was eluted with HCl (1.5M and 2.0M, 2 L). The eluate was concentrated under reduced pressure and the white residue (6.3 g) was dissolved in H_2O. The pH was adjusted to 11 with aqueous NH_3 (25%) and the solution was applied to an anion-exchange column (Dowex 1X10, 200–400 mesh, converted into $HCOO^-$ form, 80 g). The column was washed with H_2O (700 mL) and **6** was eluted with HCOOH (0.2M and 0.3M, 2 L). The eluate was evaporated to complete dryness under reduced pressure and redissolved in H_2O. Evaporation and redissolution were repeated twice more to remove any formic acid remaining. After final evaporation and drying under reduced pressure **6** was obtained as a white powder (1.1 g, 15%). ^{1}H NMR (200 MHz, D_2O [HDO 4.80 ppm]): $\delta = 2.26$ (s, 4H), 3.42 (m, 8H), 3.99 (s, 2H), 4.09 (s, 8H); MS (ESI): m/z: 421.4 $[M+H]^+$; elemental analysis calcd (%) for $C_{16}H_{27}N_3O_{10}\cdot 3HCl$ (530.9): C 36.21, H 5.70, N 7.92; found: C 35.95, H 5.93, N 8.04.

***N*,*N*″-Bis(phthalimido)diethylenetriamine-*N*′-propionic acid methyl ester (7)**: *N*,*N*″-Bis(phthalimido)diethylenetriamine (440 mg, 1.2 mmol), synthesized according to the literature,[31] was dissolved in dry DMF (10 mL) at 70 °C under an argon atmosphere. Bromopropionic methyl ester (250 mg, 1.5 mmol), anhydrous K_2CO_3 (345 mg, 2.5 mmol) and KI (42 mg, 0.25 mmol) were added successively to the stirred solution. The mixture was stirred under an argon atmosphere for 8 h at 70 °C and then evaporated to dryness. The residue was dissolved in $CHCl_3$ (10 mL) and filtered. When the filtrate had been concentrated a yellow-brown oil remained in the flask. The crude product was purified on a silica gel column (1.5 cm × 15 cm) with ethyl acetate/heptane (3:1 *v*/*v*). After removal of the solvent from the appropriate fractions ester **7** was obtained as a pale yellow solid (185 mg, 34%). $R_f = 0.50$ (silica gel, ethyl acetate/heptane 3:1 *v*/*v*); ^{1}H NMR (400 MHz, $CDCl_3$ [$CHCl_3$ 7.30 ppm]): $\delta = 2.40$ (t, 2H, $J = 7.2$ Hz), 2.84 (t, 4H, $J = 6.6$ Hz), 2.95 (t, 2H, $J = 7.2$ Hz), 3.51 (s, 3H), 3.78 (t, 4H, $J =$ 6.6 Hz), 7.69–7.83 (m, 8H).

Diethylenetriamine-*N*,*N*,*N*″,*N*″-tetraacetic-*N*′-propionic acid (H_5DTTA-prop; 8): Ester **7** (185 mg, 0.41 mmol) was heated under reflux in HCl (6M, 10 mL) for 6 h. The reaction solution was concentrated under reduced pressure to one-third of its volume and stored at 4 °C overnight. Crystallized phthalic acid was filtered off and the solution was evaporated to dryness. The residue was dissolved in a minimum of water and neutralized with NaOH (1M). The neutral solution was added to a stirred basic solution of sodium chloroacetate that had been freshly prepared by dropwise addition of NaOH (10M, 0.5 mL) to chloroacetic acid (240 mg, 2.5 mmol) in water (0.5 mL) at $T < 10$ °C. The reaction solution was stirred at 60 °C for 10 h and then cooled to room temperature. The reaction solution was set to pH ≈ 1.8 by dropwise addition of HCl (5M). The acidified solution was evaporated under reduced pressure to complete dryness. The residue was heated under reflux in dry ethanol (20 mL) for 3 min, remaining NaCl was filtered off and the solvent was removed under reduced pressure. The residue was dissolved in a minimum of water and loaded onto a cation-exchange column (Bio-Rad AG® 50W-X4, H^+ form, 1.5 cm × 7 cm). The column was washed with water until the eluate had a pH of 7 and the product mixture was eluted in one fraction with NH_3 (0.5M, 100 mL). This fraction was evaporated to dryness, dissolved in a minimum of water and loaded onto an anion-exchange column (Bio-Rad AG® 1-X4, converted into $HCOO^-$ form, 1.5 cm × 7 cm). The column was washed with water until the eluate had a pH of 7 and the product was eluted with a 0.1–2M gradient of HCOOH (total volume of eluent for gradient ≈ 400 mL). The ligand fraction eluted at approximately 1M HCOOH. The solvent was evaporated, water (50 mL) was added to dissolve the residue, and the solvent was evaporated again. The product was dried under high vacuum until all formic acid had been removed. After storage in air, **8** was obtained as a white solid (76 mg, 41%) hydrated with ca. 2.5 mol water/mol ligand. ^{1}H NMR (400 MHz, D_2O [HDO 4.80 ppm], pD ≈ 2): $\delta = 2.87$ (t, 2H, $J =$ 6.6 Hz), 3.42–3.50 (m, 10H), 3.86 (s, 8H); ^{1}H NMR (+ K_2CO_3, pD ≈ 10): $\delta = 2.38$ (t, 2H, $J = 8.2$ Hz), 2.66–2.78 (m, 8H), 2.82 (t, 2H, $J = 8.2$ Hz), 3.22 (s, 8H); MS (ESI): m/z: 408.2 $[M+H]^+$; elemental analysis calcd (%) for $C_{15}H_{25}N_3O_{10}\cdot 2.5H_2O$: C 39.82, H 6.68, N 9.29; found: C 40.1, H 6.93, N 9.02.

Potentiometry: Stock solutions of Ca^{2+}, Zn^{2+} and Cu^{2+} (20–35 mM) were prepared from chloride (Ca^{2+}, Zn^{2+}) or sulfate (Cu^{2+}) salts with double-distilled water, and standardized by complexometric titration with Na_2H_2-EDTA (Ca^{2+}, Zn^{2+}) or by gravimetry (Cu^{2+}). The $Gd(ClO_4)_3$ stock solution was made by dissolving Gd_2O_3 in a slight excess of $HClO_4$ (Merck, p.a., 60%) in double-distilled water, followed by filtering. The pH of the stock solution was adjusted to 5.5 by addition of Gd_2O_3 and its concentration was determined by titration with Na_2H_2EDTA solution using xylenol orange as indicator.

The ligand protonation constants and the stability constants of the complexes were determined at a constant ionic strength (0.1 M $(CH_3)_4NCl$). The titrations were carried out in a thermostated vessel ($25 \pm 0.2\,^{\circ}C$) using $(CH_3)_4NOH$ as titrant solution dosed with a Metrohm Dosimat 665 automatic burette. A combined glass electrode (C14/02-SC, Ag/AgCl reference electrode in 3 M KCl; Moeller Scientific Glass Instruments, Switzerland) connected to a Metrohm 692 pH/ion-meter was used to measure pH. The titrated solution (3 mL) was stirred with a magnetic stirrer and a constant N_2 flow was bubbled through it. Protonation and stability constants were determined at 0.002 – 0.003 M ligand concentrations from three or four parallel titrations. The hydrogen ion concentration was calculated from the measured pH values using the correction method suggested by Irving.[32] All protonation and stability constants were computed with the program PSEQUAD.[33]

Sample preparation: The Gd^{III} (for ^{17}O NMR, NMRD and EPR) and Eu^{III} complexes (for UV/Vis) were prepared by mixing equimolar amounts of $Gd(ClO_4)_3$ or $Eu(ClO_4)_3$ and the ligand. A slight excess (5 %) of ligand was used, and the pH was adjusted by adding $HClO_4$ or NaOH (each 0.1 M). The solution was allowed to react for 12 h at room temperature. The absence of free metal was checked in each sample by testing with xylenol orange for complex solutions of pH ≈ 6 or with a mixture of eriochrom black T and methyl orange for complex solutions of pH ≈ 9. ^{17}O-enriched water (Isotec, ^{17}O: 11.4 %) was added to the solutions for the ^{17}O NMR measurements to improve the sensitivity and the pH was checked again. The concentrations and pH values of the solutions used were as follows. $[Gd(eptpa\text{-}bz\text{-}NO_2)(H_2O)]^{2-}$: 0.0558 mol kg^{-1}, pH 6.0 (^{17}O NMR, EPR); 0.00535 M, pH 6.0 (NMRD). $[Gd(eptpa)(H_2O)]^{2-}$: 0.0325 mol kg^{-1}, pH 6.4 (variable-temperature ^{17}O NMR); 0.069 mol kg^{-1}, pH 6.2 (variable pressure ^{17}O NMR); 0.080 M (EPR). $[Gd(dptpa)]^{2-}$: 0.0320 mol kg^{-1}, pH 9.0 (^{17}O NMR, EPR); 0.015 M, pH 9.0 (NMRD). $[Eu(eptpa\text{-}bz\text{-}NO_2)(H_2O)]^{2-}$: 0.01913 M, pH 6.0 (UV/Vis). $[Gd(dtta\text{-}prop)(H_2O)]^{2-}$: 0.0221 mol kg^{-1}, pH 9.2 (^{17}O NMR).

UV/Vis spectroscopy: The absorbance spectra of $[Eu^{III}(eptpa\text{-}bz\text{-}NO_2)]$ were recorded at 25 and 68 °C on a Perkin – Elmer Lambda 19 spectrometer. The measurements were done in thermostated cells with a 10 cm optical pathlength at $\lambda = 577.5 - 581.5$ nm.

^{17}O NMR measurements: Variable-temperature ^{17}O NMR measurements were performed on a Bruker AM-400 (9.4 T, 54.2 MHz) spectrometer and a Bruker VT-1000 temperature control unit was used to stabilize the temperature, which was measured by a substitution technique. The samples were sealed in glass spheres that fitted into 10 mm NMR tubes, to eliminate susceptibility corrections to the chemical shifts.[34] Longitudinal relaxation rates $1/T_1$ were obtained by the inversion recovery method, and transverse relaxation rates $1/T_2$ by the Carr – Purcell – Meiboom – Gill spin – echo technique. As an external reference, a solution of the corresponding $Y^{III}L$ complex of the same concentration and pH as the $Gd^{III}L$ sample (L = EPTPA-bz-NO_2, DPTPA) or acidified water of pH 3.4 (for the measurements on $[Gd(dtta\text{-}prop)(H_2O]^{2-}$) was used.

Variable-pressure ^{17}O NMR measurements up to 200 MPa pressure were performed on a Bruker ARX-400 spectrometer equipped with a home-built high-pressure probe head. The temperature was controlled by circulating fluid from a temperature bath, and was measured by means of a built-in Pt resistor. The pressure dependence of the transverse relaxation rate of acidified water, used as a reference, was described by assuming an activation volume of $+0.97$ cm^3 mol^{-1}.[35]

NMRD: The $1/T_1$ NMRD profiles were obtained on a Stelar Spinmaster FFC fast field cycling NMR relaxometer covering a continuum of magnetic fields from 5×10^{-4} to 0.47 T (corresponding to a proton Larmor frequency range 0.022 – 20 MHz).

ESR: The X-band EPR spectra were recorded on a Bruker ESP 300 spectrometer (9.425 GHz, 0.34 T). High-field spectra on $[Gd(eptpa)(H_2O)]^{2-}$ were obtained on a home-built spectrometer (Department of Experimental Physics, Technical University of Budapest, Hungary), in which a frequency-stabilized Gunn diode oscillator was used at 75 GHz base frequency, followed by a frequency tripler for the 225 GHz measurements (8.1 T). A PTFE sample holder contained the aqueous sample, which was placed in an oversized waveguide so that no resonant cavities would be used. The transverse electronic relaxation rates $1/T_{2e}$ at various temperatures were obtained from the EPR linewidths according to Reuben's method.[36]

Data analysis: ^{17}O NMR, NMRD and EPR data were analyzed either with a program working on a Matlab platform, version 5.3,[37] or with Scientist® for Windows® by Micromath®, version 2.0. The reported errors correspond to one standard deviation obtained by the statistical analysis.

Appendix

Oxygen-17 NMR: From the measured ^{17}O NMR relaxation rates and angular frequencies of the paramagnetic solutions $1/T_1$, $1/T_2$ and ω, and of the reference $1/T_{1A}$, $1/T_{2A}$ and ω_A, one can calculate the reduced relaxation rates and chemical shift $1/T_{1r}$, $1/T_{2r}$ and ω_r, which may be written as in Equations (A1) – (A3), where P_m is the molar fraction of bound water, $1/T_{1m}$ and $1/T_{2m}$ are the relaxation rates of the bound water, and $\Delta\omega_m$ is the chemical shift difference between bound and bulk water.

$$\frac{1}{T_{1r}} = \frac{1}{P_m}\left[\frac{1}{T_1} - \frac{1}{T_{1A}}\right] = \frac{1}{T_{1m} + \tau_m} \tag{A1}$$

$$\frac{1}{T_{2r}} = \frac{1}{P_m}\left[\frac{1}{T_2} - \frac{1}{T_{2A}}\right] = \frac{1}{\tau_m}\frac{T_{2m}^{-2} + \tau_m^{-1}T_{2m}^{-1} + \Delta\omega_m^2}{(\tau_m^{-1} + T_{2m}^{-1})^2 + \Delta\omega_m^2} \tag{A2}$$

$$\Delta\omega_r = \frac{1}{P_m}(\omega - \omega_A) = \frac{\Delta\omega_m}{(1 + \tau_m T_{2m}^{-1})^2 + \tau_m^2\Delta\omega_m^2} + \Delta\omega_{os} \tag{A3}$$

ω_m is determined from the hyperfine or scalar coupling constant, $A/\hbar$, according to Equation (A4), where B represents the magnetic field, S is the electron spin and g_L is the isotropic Landé g factor.

$$\Delta\omega_m = \frac{g_L\,\mu_B\,S(S+1)\,B}{3\,k_B\,T}\,\frac{A}{\hbar} \tag{A4}$$

The outer-sphere contribution to the chemical shift is assumed to be linearly related to $\Delta\omega_m$ by a constant C_{os} [Eq. (A5)].

$$\Delta\omega = C_{os}\Delta\omega_m \tag{A5}$$

The ^{17}O longitudinal relaxation rates are given by Equation (A6), where γ_S and γ_I are the electronic and nuclear gyromagnetic ratios respectively ($\gamma_S = 1.76 \times 10^{11}$ rad s^{-1}T^{-1}, $\gamma_I = -3.626 \times 10^7$ rad s^{-1}T^{-1}), r is the effective distance between the electron charge and the ^{17}O nucleus, I is the nuclear spin (5/2 for ^{17}O), χ is the quadrupolar coupling constant, η is an asymmetry parameter [Eq. (A6)]:

$$\frac{1}{T_{1m}} = \left[\frac{1}{15}\left(\frac{\mu_0}{4\pi}\right)^2\frac{\hbar^2\gamma_I^2\gamma_S^2}{r_{GdO}^6}S(S+1)\right] \times \left[6\tau_{d1} + 14\frac{\tau_{d2}}{1+\omega_S^2\tau_{d2}^2}\right] + \frac{3\pi^2}{10}\frac{2I+3}{I^2(2I-1)}\chi^2(1+\eta^2/3)\tau_{RO} \tag{A6}$$

where:

$$\frac{1}{\tau_{di}} = \frac{1}{\tau_m} + \frac{1}{\tau_{RO}} + \frac{1}{T_{ie}} \qquad \text{for } i = 1, 2 \tag{A7}$$

The τ_{RO} overall rotational correlation time is assumed to have a simple exponential temperature dependence with an E_R activation energy as given in Equation (A8).

$$\tau_{RO} = \tau_{RO}^{298}\exp\left[\frac{E_R}{R}\left(\frac{1}{T} - \frac{1}{298.15}\right)\right] \tag{A8}$$

In the transverse relaxation the scalar contribution $1/T_{2sc}$ is the most important [Eq. (A9)]. Here $1/\tau_{s1}$ is the sum of the exchange rate constant and the electron spin relaxation rate.

$$\frac{1}{T_{2m}} \cong \frac{1}{T_{2sc}} = \frac{S(S+1)}{3}\left(\frac{A}{\hbar}\right)^2\tau_{s1} \tag{A9}$$

$$\frac{1}{\tau_{s1}} = \frac{1}{\tau_m} + \frac{1}{T_{1e}} \tag{A10}$$

The inverse binding time (or exchange rate, k_{ex}) of water molecules in the inner sphere is assumed to obey the Eyring equation [Eq. (A11)], where ΔS^{+} and ΔH^{+} are the entropy and enthalpy of activation for the exchange, and k_{298}^{ex} is the exchange rate at 298.15 K.

$$\frac{1}{\tau_m}=k_{ex}=\frac{k_B T}{h}\exp\left[\frac{\Delta S^{+}}{R}-\frac{\Delta H^{+}}{RT}\right]=\frac{k_{ex}^{298}\,T}{298.15}\exp\left[\frac{\Delta H^{+}}{R}\left(\frac{1}{298.15}-\frac{1}{T}\right)\right] \quad (A11)$$

The electron spin relaxation rates $1/T_{1e}$ and $1/T_{2e}$ for metal ions in solution with $S>1/2$ are mainly governed by a transient zero-field-splitting mechanism (ZFS).[38] The ZFS term is expressed by Equations (A12) and (A13), where Δ^2 is the trace of the square of the transient zero-field-splitting tensor, τ_v is the correlation time for the modulation of the ZFS with activation energy E_v, ω_s is the Larmor frequency of the electron spin.

$$\left(\frac{1}{T_{1e}}\right)^{ZFS}=\frac{1}{25}\Delta^2\tau_V\{4S(S+1)-3\}\left(\frac{1}{1+\omega_S^2\tau_V^2}+\frac{4}{1+4\omega_S^2\tau_V^2}\right) \quad (A12)$$

$$\left(\frac{1}{T_{2e}}\right)^{ZFS}=\Delta^2\,\tau_V\left[\frac{5.26}{1+0.372\,\omega_S^2\,\tau_V^2}+\frac{7.18}{1+1.24\,\omega_S\,\tau_V}\right] \quad (A13)$$

$$\tau_V=\tau_V^{298}\exp\left[\frac{E_v}{R}\left(\frac{1}{T}-\frac{1}{298.15}\right)\right] \quad (A14)$$

The pressure dependence of $\ln k_{ex}$ is linear [Eq. (A15)], where ΔV^{+} is the activation volume and $(k_{ex})_0^T$ is the water exchange rate at zero pressure and temperature T.

$$\frac{1}{\tau_m}=k_{ex}=(k_{ex})_0^T\exp\left[-\frac{\Delta V^{+}}{RT}P\right] \quad (A15)$$

NMRD: The measured proton relaxivities (normalized to 1 mM Gd^{III} concentration) contain both inner- and outer-sphere contributions:

$$r_1=r_{1is}+r_{1os} \quad (A16)$$

The inner-sphere term is given by Equation (A17), where q is the number of inner-sphere water molecules.

$$r_{1is}=\frac{1}{1000}\times\frac{q}{55.55}\times\frac{1}{T_{1m}^{H}+\tau_m} \quad (A17)$$

The longitudinal relaxation rate of inner-sphere protons $1/T_{1m}^{H}$ is expressed by Equation (A18):

$$\frac{1}{T_{1m}^{H}}=\frac{2}{15}\left(\frac{\mu_0}{4\pi}\right)^2\frac{\hbar^2\gamma_S^2\gamma_I^2}{r_{GdH}^6}S(S+1)\left[\frac{3\tau_{d1H}}{1+\omega_I^2\tau_{d2H}^2}\right] \quad (A18)$$

where r_{GdH} is the effective distance between the Gd^{III} electron spin and the water protons, ω_I is the proton resonance frequency and τ_{diH} is given by Equation (A19), where τ_{RH} is the rotational correlation time of the Gd^{III}–H_{water} vector.

$$\frac{1}{\tau_{diH}}=\frac{1}{\tau_m}+\frac{1}{\tau_{RH}}+\frac{1}{T_{ie}}\qquad \text{for } i=1,2 \quad (A19)$$

The outer-sphere contribution is described by Equation (A20), where N_A is the Avogadro constant and J_{os} is a spectral density function given by Equation (A21), with $j=1,2$.

$$r_{1os}=\frac{32\,N_A\pi}{405}\left(\frac{\mu_0}{4\pi}\right)^2\frac{\hbar^2\gamma_S^2\gamma_I^2}{a_{GdH}D_{GdH}}S(S+1)\left[3J_{os}(\omega_I,T_{1e})+7J_{os}(\omega_S,T_{2e})\right] \quad (A20)$$

$$J_{os}(\omega,T_{je})=\mathrm{Re}\left[\frac{1+1/4\left(i\omega\tau_{GdH}+\frac{\tau_{GdH}}{T_{je}}\right)^{1/2}}{1+\left(i\omega\tau_{GdH}+\frac{\tau_{GdH}}{T_{je}}\right)^{1/2}+4/9\left(i\omega\tau_{GdH}+\frac{\tau_{GdH}}{T_{je}}\right)+1/9\left(i\omega\tau_{GdH}+\frac{\tau_{GdH}}{T_{je}}\right)^{3/2}}\right] \quad (A21)$$

A value of 3.6 Å was used for a_{GdH}. For the temperature dependence of the diffusion coefficient D_{GdH} for the diffusion of a water proton away from a Gd^{III} complex, we have assumed an exponential temperature dependence, with an activation energy E_{DGdH} [Eq. (A22)].

$$D_{GdH}=D_{GdH}^{298}\exp\left[\frac{E_{D\,GdH}}{R}\left(\frac{1}{T}-\frac{1}{298.15}\right)\right] \quad (A22)$$

Acknowledgements

We are grateful to Prof. András Jánossy and his co-workers, Technical University of Budapest, for the high-field EPR measurements. We also thank Prof. Manfred Mutter and his co-workers, EPFL, for the MS spectra. This research was supported financially by the Swiss National Science Foundation and the Office for Education and Science (OFES) and was carried out in the framework of the EC COST Action D18.

[1] *The Chemistry of Contrast Agents in Medical Magnetic Resonance Imaging* (Eds.: É. Tóth, A. E. Merbach), Wiley, Chichester, **2001**.
[2] S. Aime, C. Cabella, S. Colombatto, S. G. Crich, E. Gianolio, F. Maggioni, *J. Magn. Reson. Imaging* **2002**, *16*, 394.
[3] A. D. Nunn, K. E. Linder, M. F. Tweedle, *Q. J. Nucl. Med.* **1997**, *41*, 155.
[4] V. Jacques, J. F. Desreux, *Top. Curr. Chem.* **2002**, *221*, 123.
[5] É. Tóth, L. Helm, A. E. Merbach, in *The Chemistry of Contrast Agents in Medical Magnetic Resonance Imaging* (Eds.: É. Tóth, A. E. Merbach), Wiley, Chichester, **2001**, p. 45.
[6] S. M. Cohen, J. Xu, E. Radkov, K. N. Raymond, M. Botta, A. Barge, S. Aime, *Inorg. Chem.* **2000**, *39*, 5747.
[7] S. Aime, A. Barge, M. Botta, J. A. Howard, R. Kataky, M. P. Lowe, J. M. Moloney, D. Parker, A. S. de Sousa, *Chem. Commun.* **1999**, 1047.
[8] D. Pubanz, G. Gonzalez, D. H. Powell, A. E. Merbach, *Inorg. Chem.* **1995**, *34*, 4447.
[9] R. Ruloff, É. Tóth, R. Scopelliti, R. Tripier, H. Handel, A. E. Merbach, *Chem. Commun.* **2002**, 2630.
[10] G. Ruser, W. Ritter, H. R. Maecke, *Bioconjugate Chem.* **1990**, *1*, 345.
[11] Y.-M. Wang, C.-H. Lee, G.-C. Liu, R.-S. Sheu, *Dalton Trans.* **1998**, 4113.
[12] T.-H. Cheng, Y.-M. Wang, K.-T. Lin, G.-C. Liu, *Dalton Trans.* **2001**, 3357.
[13] V. F. Vasileva, O. Y. Lavrova, N. M. Dyatlova, V. G. Yashunskii, *Zh. Obshch. Khim*. **1966**, *36*, 674.
[14] J. D. Clark, D. Q. Perrin, *Q. Rev.* **1964**, *18*, 295.
[15] P. Letkeman, A. E. Martell, *Inorg. Chem.* **1979**, *18*, 1284.
[16] T.-H. Cheng, T.-M. Lee, M.-H. Ou, C.-R. Li, G.-C. Liu, Y.-M. Wang, *Helv. Chim. Acta* **2002**, *85*, 1033.
[17] T. J. McMurry, C. G. Pippin, C. Wu, K. A. Deal, M. W. Brechbiel, S. Mirzadeh, O. A. Gansow, *J. Med. Chem.* **1998**, *41*, 3546.
[18] A. E. Martell, R. J. Motekaitis, E. T. Clarke, R. Delgado, Y. Sun, R. Ma, *Supramol. Chem.* **1996**, *6*, 353.
[19] D. J. Sawyer, J. E. Powell, *Polyhedron* **1989**, *8*, 1425.
[20] M. F. Tweedle, J. J. Hagan, K. Kumar, S. Mantha, C. A. Chang, *Magn. Reson. Imaging* **1991**, *9*, 409.
[21] N. Graeppi, D. H. Powell, G. Laurenczy, L. Zékány, A. E. Merbach, *Inorg. Chim. Acta* **1995**, *235*, 311.
[22] F. A. Dunand, A. Borel, A. E. Merbach, *J. Am. Chem. Soc.* **2002**, *124*, 710.
[23] F. Yerly, K. I. Hardcastle, L. Helm, S. Aime, M. Botta, A. E. Merbach, *Chem. Eur. J.* **2002**, *8*, 1031.
[24] a) S. Rast, A. Borel, L. Helm, E. Belorizky, P. H. Fries, A. E. Merbach, *J. Am. Chem. Soc.* **2001**, *123*, 2637; b) S. Rast, P. H. Fries, E. Belorizky, A. Borel, L. Helm, A. E. Merbach, *J. Chem. Phys.* **2001**, *115*, 7554.
[25] F. Dunand, A. Borel, L. Helm, *Inorg. Chem. Commun.* **2002**, *5*, 811.
[26] a) A. D. McLachlan, *Proc. R. Soc. London A* **1964**, *280*, 271; b) D. H. Powell, A. E. Merbach, G. González, E. Brücher, K. Micskei, M. F. Ottaviani, K. Köhler, A. von Zelewsky, O. Y. Grinberg, Y. S. Lebedev, *Helv. Chim. Acta* **1993**, *76*, 2129.
[27] L. Helm, É. Tóth, A. E. Merbach, in *Metals in Biology* (Ed.: H. Siegel), Marcel Dekker, New York, **2003**, p. 589.

[28] S. F. Lincoln, A. E. Merbach, *Adv. Inorg. Chem.* **1995**, *42*, 1.
[29] C. Cossy, L. Helm, A. E. Merbach, *Inorg. Chem.* **1989**, *28*, 2699.
[30] J. P. Dubost, J. M. Leger, M. H. Langlois, D. Meyer, M. Schaefer, *C.R. Acad. Sci. Paris* **1991**, *312*, 349.
[31] C.-Y. Ng, R. J. Motekaitis, A. E. Martell, *Inorg. Chem.* **1979**, *18*, 2982.
[32] H. Irving, M. G. Miles, L. Pettit, *Anal. Chim. Acta* **1967**, *38*, 475.
[33] L. Zékány, I. Nagypál, in *Computational Methods for Determination of Formation Constants* (Ed.: D. J. Leggett), Plenum Press, New York, **1985**, p. 291.
[34] A. D. Hugi, L. Helm, A. E. Merbach, *Helv. Chim. Acta* **1985**, *68*, 508.
[35] Y. Ducommun, W. L. Earl, A. E. Merbach, *Inorg. Chem.* **1979**, *18*, 2754.
[36] J. Reuben, *J. Phys. Chem.* **1971**, *75*, 3164.
[37] F. Yerly, *VISUALISEUR* 2.2.4. and *OPTIMISEUR* 2.2.4, Institute of Molecular and Biological Chemistry, University of Lausanne, Switzerland, **1999**.
[38] a) A. D. McLachlan, *Proc. R. Soc. London A* **1964**, *280*, 271; b) D. H. Powell, A. E. Merbach, G. González, E. Brücher, K. Micskei, M. F. Ottaviani, K. Köhler, A. von Zelewsky, O. Y. Grinberg, Y. S. Lebedev, *Helv. Chim. Acta* **1993**, *76*, 2129.
[39] *IUPAC Stability Constants*, Academic Software and K. J. Powell, Release 1.05, Yorks, LS21 2PW (UK), **1999**.
[40] C. Paul-Roth, K. N. Raymond, *Inorg. Chem.* **1995**, *34*, 1408.
[41] D. H. Powell, O. M. Ni Dhubhghaill, D. Pubanz, L. Helm, Y. S. Lebedev, W. Schlaepfer, A. E. Merbach, *J. Am. Chem. Soc.* **1996**, *118*, 9333.

Received: November 25, 2002 [F4612]